DYNAMIC CHARACTERISTICS OF HIGHLY COMPLIANT GRAPHITE REINFORCED CEMENTITIOUS COMPOSITE PLATES

Teng K. Ooi
Adjunct Faculty Member
Department of Mechanical and Aerospace Engineering
University of Alabama in Huntsville
Huntsville, AL 35899

Robert E. Vaughan
Aerospace Engineer
Aviation Engineering Directorate
Structures and Materials Division
Redstone Arsenal, AL 35898

John A. Gilbert
Professor of Mechanical Engineering
Department of Mechanical and Aerospace Engineering
University of Alabama in Huntsville
Huntsville, AL 35899

Robert C. Engberg
Aerospace Engineer
ED27/Structural & Dynamics Test Group
NASA, Marshall Space Flight Center
MSFC, AL 35812

Mark V. Bower
Assistant Dean of Engineering and Associate Professor
Department of Mechanical and Aerospace Engineering
University of Alabama in Huntsville
Huntsville, AL 35899

ABSTRACT

This paper describes how finite element and experimental modal analysis can be used to characterize the dynamic behavior of plates made from a new class of **P**olymer-**E**nhanced, **G**raphite **R**einforced **C**ementitious **C**omposite (**PEGRCC**) materials. A good agreement is obtained between both methods and results show that PEGRCC materials can be modeled and tested using tools similar to those applied to study classical composite laminates.

INTRODUCTION

A limited number of static tests have been performed to determine the material properties of graphite reinforced cementitious composites [1,2]. This paper describes how finite element and experimental modal analysis can be used to characterize the dynamic behavior of plates made from these materials. The results will help researchers to predict the dynamic response of large structures fabricated from these plates.

Finite element models were developed based on classical laminated plate theory. Experimental tests began by studying five plates having the same aspect ratio to determine how the uncertainties in the material properties due to a large number of variables associated with the fabrication process affected modal parameters. Then, plates with aspect ratios from 0.5 to 4.5 were impact tested in a free-hanging configuration to determine their natural frequencies and mode shapes.

The experimental test results were compared to those obtained from finite element analyses to validate the finite element models. Results show that PEGRCC materials can be modeled and tested using tools similar to those applied to study classical composite laminates.

PEGRCC PLATE FABRICATION

A large 81.3 cm x 142.2 cm PEGRCC plate was fabricated by placing the cementitious mixture described in Figure 1 over three layers of graphite. Test plates having different aspect ratios were later cut from this plate.

According to the manufacturer, each layer of reinforcement consisted of a non-impregnated graphite mesh with 3,000 fibers

per tow, spaced at 3.18 mm intervals. Each tow is 0.19 mm thick by 1.07 mm wide; the elastic modulus and tensile strength of the graphite are 231 GPa and 3.65 GPa, respectively.

The mixture was prepared by first mixing the cement and micro-bubbles. Then the acrylic fortifier, latex, and water were added to produce a mixture having a smooth texture.

The plate was fabricated by placing the first layer of graphite reinforcement [90°, 90°] on top of a plexi-glass sheet. Wires having a thickness of 2.54 mm were affixed at 7.62 cm intervals over the mesh and the mixture was placed over this configuration. After 12 hours, the wires were removed and the grooves filled with the mixture. This process was repeated for the remaining layers, making sure not to place wires over the same locations used while constructing the previous layer. After letting the plate cure for seven days, it was cut into smaller plates having different aspect ratios.

Ingredient	% Mass weight
K-25 micro-bubbles	11.75
Portland cement	30.06
Latex	16.70
Acrylic fortifier	8.08
Water	33.41

Figure 1. Mix proportions.

PEGRCC LAMINATE CONSTITUTIVE EQUATIONS

The constitutive equations that relate the force and moment resultants to the strains for PEGRCC anisotropic plates can be derived based on the classical laminated plate theory and may be written as:

$$\begin{bmatrix} N_x \\ N_y \\ N_{xy} \\ M_x \\ M_y \\ M_{xy} \end{bmatrix} = \begin{bmatrix} A_{11} & A_{12} & A_{13} & B_{11} & B_{12} & B_{13} \\ A_{21} & A_{22} & A_{23} & B_{21} & B_{22} & B_{23} \\ A_{31} & A_{32} & A_{33} & B_{31} & B_{32} & B_{33} \\ B_{11} & B_{12} & B_{13} & D_{11} & D_{12} & D_{13} \\ B_{21} & B_{22} & B_{23} & D_{21} & D_{22} & D_{23} \\ B_{31} & B_{32} & B_{33} & D_{31} & D_{32} & D_{33} \end{bmatrix} \begin{bmatrix} \varepsilon_{0x} \\ \varepsilon_{0y} \\ \gamma_{0xy} \\ K_x \\ K_y \\ K_{xy} \end{bmatrix}$$

where $(A_{ij}, B_{ij}, D_{ij}) = \sum_{r=1}^{N} \int_{Z_r}^{Z_{r+1}} Q_{ij}^{(r)} (1, z, z^2) dz$ and

N_x, N_y, N_{xy} = resultant force and shear force in x-axis, y-axis, and x-y plane, respectively

M_x, M_y, M_{xy} = resultant moment and twisting about x-axis, y-axis, and x-y plane, respectively

Z_r, Z_{r+1} = thickness coordinates of the lower and the upper surface of the r-th ply

$Q_{ij}^{(r)}$ = material stiffnesses of the r-th ply

Z = laminate transverse direction, normal to x-y plane

N = number of plies in the laminate

ε_{0x} = midplane strain in x-axis

ε_{0xy} = midplane strain in y-axis

γ_{0xy} = midplane shear strain in x-y plane

K_x = plate bending curvature in the x-z plane

K_y = plate bending curvature in the y-z plane

K_{xy} = plate twisting curvature in the x-y plane

A_{ij} = extensional stiffnesses

B_{ij} = bending-extension coupling stiffnesses

D_{ij} = bending stiffnesses

The *A*, *B*, and *D* matrices are computed based on the laminate material properties, geometry, and stacking sequence. For a three-ply specially orthotropic laminate (laminate whose principal material axes are aligned with the natural body axes), these matrices were computed based on previously obtained material properties [1,2]. In this configuration, the bending-extensional coupling coefficients, B_{ij}, the bending-twisting coefficients, D_{13}, D_{23}, and the shear-extensional coupling coefficients, A_{13}, A_{23}, are all zero.

The material properties are 3.48 GPa for the elastic modulus, 517 MPa for the shear modulus, 0.137 for the Poisson's ratio, and 657 kg/m^3 for the mass density. Each ply is assumed to have a thickness of 2.54 mm.

FINITE ELEMENT ANALYSIS OF PEGRCC PLATES

Finite element models for PEGRCC laminated plates were developed based on the classical laminated plate theory. The models were generated using physical dimensions and the material properties mentioned above. MSC/Nastran was selected as the finite element code because of its multi-layered composite element capabilities for normal mode analysis.

Each model consisted of equally spaced quadrilateral membrane-bending plate elements with uniform thickness. Damping was neglected in the analysis and refinements in element sizes were made until the natural frequencies converged.

Only the lower natural frequencies and their associated mode shapes are of interest because they adequately describe the dynamic behavior of the laminate. Figure 2, for example, shows the first four mode shapes predicted for a 152.40 mm x 228.60 mm PEGRCC plate; the corresponding natural frequencies are included in the figure caption.

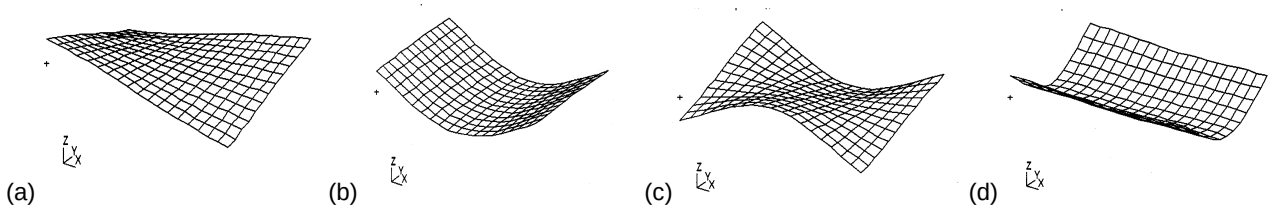

Figure 2. Finite element results for a 152.4 mm x 228.6 mm PEGRCC plate, (a) 1st mode, frequency =269.50 Hz, (b) 2nd mode, frequency = 410.86 Hz, (c) 3rd mode, frequency = 674.20 Hz, (d) 4th mode, frequency = 913.14 Hz.

EXPERIMENTAL TESTING OF PEGRCC PLATES

Modal testing was conducted to validate the finite element models. Test plates were struck with an impact hammer while they were suspended by elastic cords in the free-hanging configuration and frequency response functions (FRFs), such as those depicted in Figure 3, were measured over an array of points using an accelerometer. Mode shapes and natural frequencies (see Figure 4) were determined using the Rational Fraction Polynomial method.

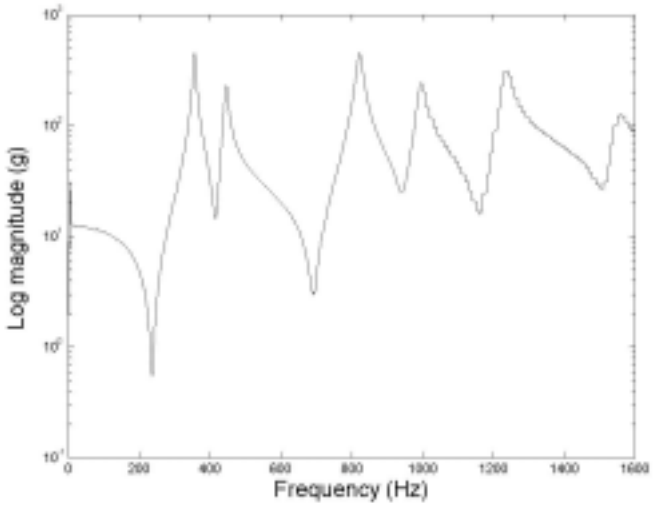

Figure 3. Drive point FRF for a 152.4 mm x 228.6 mm PEGRCC plate.

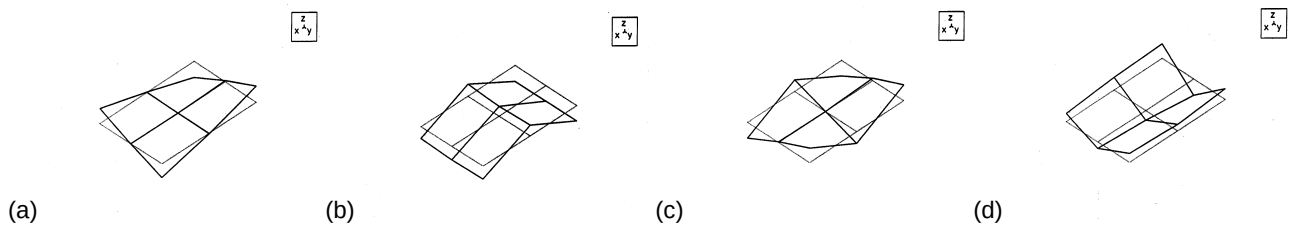

Figure 4. Experimental results for a 152.4 mm x 228.6 mm PEGRCC plate, (a) 1st mode, frequency = 342.11 Hz, (b) 2nd mode, frequency = 426.64 Hz, (c) 3rd mode, frequency = 799.43 Hz, (d) 4th mode, frequency = 993.47 Hz.

During the experiments, measurements were made in the transverse direction (z-axis) only, over a relatively coarse array. Typically, the experimental and finite element mode shapes agreed very well but the natural frequencies did not.

Five, 152.40 mm x 228.60 mm plates were initially tested to investigate how variations created during the fabrication process affected the dynamic characteristics. Figure 5 shows the natural frequencies for the first three modes and their corresponding mean frequencies and standard deviations.

From statistical analysis, the interval that contains 90% of the parent population frequencies with 90% confidence is 321.85 Hz to 356.79 Hz. It can be seen that the five measured values fall within this range thereby illustrating that adequate control over the plate fabrication process exists.

Mode	1st Plate Freq., Hz	2nd Plate Freq., Hz	3rd Plate Freq., Hz	4th Plate Freq., Hz	5th Plate Freq., Hz	Mean Freq., Hz	Standard Deviation, Hz
1st mode	342.11	345.50	340.00	339.00	330.00	339.32	5.78
2nd mode	426.64	432.50	426.00	421.00	410.00	423.23	8.44
3rd mode	799.43	805.50	799.00	793.00	778.00	794.99	10.48

Figure 5. Results for five 152.40 mm x 228.60 mm plates.

Tests were conducted on plates having aspect ratios from 0.5 to 4.5. Figures 6, 8, and 10 show comparisons between experimental results and finite element predictions for the first three modes, respectively, while Figures 7, 9, and 11 show plots of frequency variations with aspect ratio for these modes, respectively.

Plate Size (mm x mm)	Thickness (mm)	Aspect Ratio	Experimental Frequency (Hz)	Finite Element Frequency (Hz)	% Difference
152.40 x 76.20	9.449	0.50	949.00	714.02	-24.76
152.40 x 101.60	8.941	0.67	657.12	520.36	-20.81
152.40 x 152.40	9.525	1.00	489.07	394.30	-19.38
152.40 x 228.60	9.677	1.50	342.11	269.50	-21.22
152.40 x 304.80	9.652	2.00	242.36	220.76	-8.91
152.40 x 381.00	10.109	2.50	152.38	148.38	-2.63
152.40 x 457.20	9.652	3.00	102.75	106.39	3.54
152.40 x 533.40	9.855	3.50	80.16	73.63	-8.15
152.40 x 609.60	9.754	4.00	59.34	55.96	-5.70
152.40 x 685.80	10.008	4.50	46.00	45.27	-1.59
				Mean % Absolute Discrepancy	11.67

Figure 6. Data obtained for 1st (fundamental) mode.

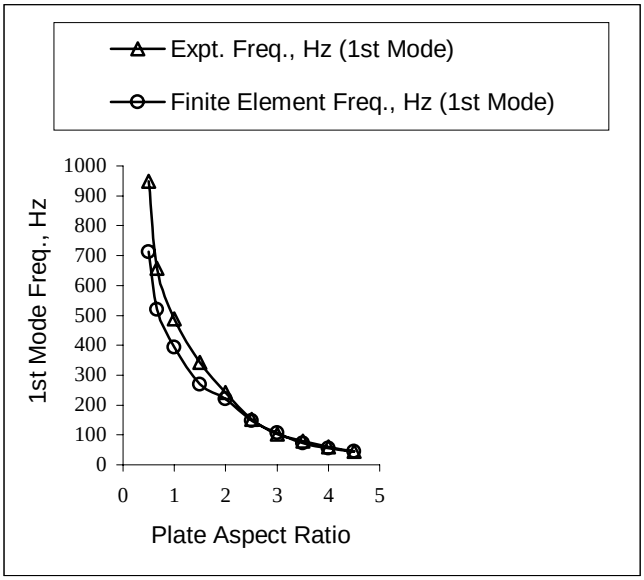

Figure 7. Frequency variations observed for 1st (fundamental) mode.

Plate Size (mm x mm)	Thickness (mm)	Aspect Ratio	Experimental Frequency (Hz)	Finite Element Frequency (Hz)	% Difference
152.40 x 76.20	9.449	0.50	1024.75	841.00	-17.93
152.40 x 101.60	8.941	0.67	861.62	794.17	-7.83
152.40 x 152.40	9.525	1.00	958.26	849.20	-11.38
152.40 x 228.60	9.677	1.50	426.64	410.86	-3.70
152.40 x 304.80	9.652	2.00	248.17	190.75	-23.14
152.40 x 381.00	10.109	2.50	205.28	158.52	-22.78
152.40 x 457.20	9.652	3.00	163.31	135.44	-17.07
152.40 x 533.40	9.855	3.50	148.11	108.65	-26.64
152.40 x 609.60	9.754	4.00	128.23	93.95	-26.73
152.40 x 685.80	10.008	4.50	113.00	85.15	-24.65
				Mean % Absolute Discrepancy	18.19

Figure 8. Data obtained for 2nd mode.

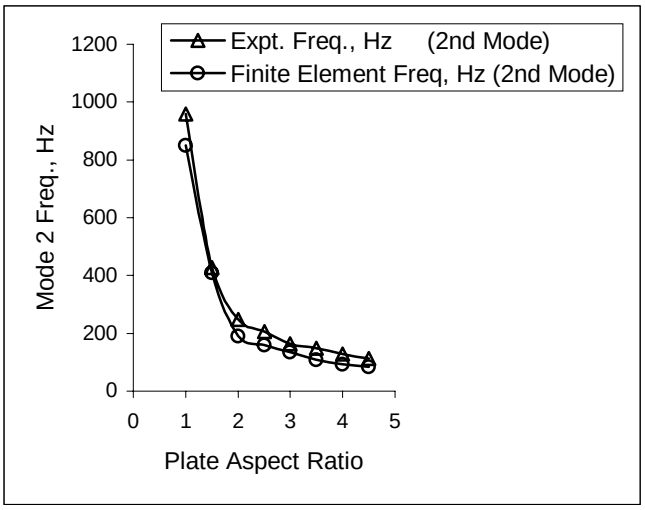

Figure 9. Frequency variations observed for 2nd mode.

Plate Size (mm x mm)	Thickness (mm)	Aspect Ratio	Experimental Frequency (Hz)	Finite Element Frequency (Hz)	% Difference
152.40 x 76.20	9.449	0.50	1623.80	1623.70	-0.01
152.40 x 101.60	8.941	0.67	1543.92	1284.40	-16.81
152.40 x 152.40	9.525	1.00	1292.66	933.05	-27.82
152.40 x 228.60	9.677	1.50	799.43	674.20	-15.66
152.40 x 304.80	9.652	2.00	556.76	443.54	-20.34
152.40 x 381.00	10.109	2.50	450.11	354.39	-21.27
152.40 x 457.20	9.652	3.00	287.08	291.88	1.67
152.40 x 533.40	9.855	3.50	223.41	202.25	-9.47
152.40 x 609.60	9.754	4.00	162.71	153.89	-5.42
152.40 x 685.80	10.008	4.50	130.00	124.55	-4.19
				Mean % Absolute Discrepancy	12.27

Figure 10. Data obtained for 3rd mode.

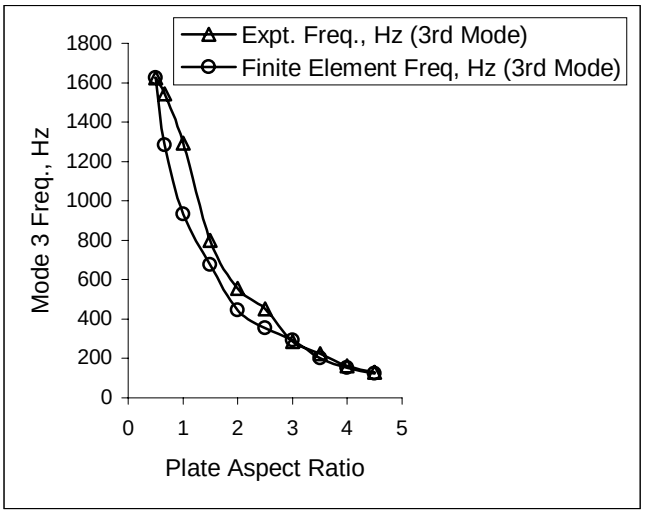

Figure 11. Frequency variations observed for 3rd mode.

DISCUSSION

A good agreement is observed between the experimental results and the finite element predictions indicating that the material properties used in the finite element models are valid. The mean absolute discrepancies between the experimental and the finite element natural frequencies are 11% for the 1st mode, 18% for 2nd mode, and 12% for 3rd mode. In all cases, the finite element analysis underpredicts the natural frequencies when compared to the experimental values. These discrepancies could be due to slight non-uniformities in the material properties and variations in geometric dimensions of the plates.

Figure 7, 9, and 11 show the effect of frequency variation of the experimental and the finite element natural frequency for the free-free PEGRCC plates with various aspect ratios for the first 3 modes. The frequencies are highly dependent on the aspect ratios and decrease when the aspect ratio increases from 0.5 to 4.5. When the aspect ratio is greater than 4.5, the frequencies appear to taper-off and approach a constant value. These results are typical of specially orthotropic laminated composite plates and they provide a better understanding of the dynamic behavior of PEGRCC laminated plates required for predicting the structural response, generating design data, and parametric studies.

A frequency shift of approximately 3% was observed due to the mass loading of the 0.0017 kg accelerometer employed for testing. The smaller plates exhibited more deviations in the frequency shift than the larger plates due to their lower masses.

Another frequency shift was noted when additional tests were conducted two weeks after the initial tests were performed. The additional curing time and the hydration of the PEGRCC materials stiffened the plates and caused the frequency to increase by approximately 3%.

CONCLUSIONS

The good agreement between the experimental modal parameters and the finite element predictions indicates that standard impact modal testing can be applied to study PEGRCC materials. The accuracy of the finite element analysis shows that the finite element model based on the classical laminated plate theory is valid. Since PEGRCC materials behave like classical composite materials and the classical mechanics of composite material theory is applicable, it should be possible to predict the dynamic response of PEGRCC laminated structures using the finite element model developed in this paper.

ACKNOWLEDGEMENTS

The authors would like to thank NASA, the US Air Force, and the US Army for providing the facilities and resources that made this research possible.

REFERENCES

[1] Vaughan, R.E., Gilbert, J.A., “Analysis of graphite reinforced cementitious composites," Proc. of the 2001 SEM Annual Conference and Exposition, Portland, Oregon, June 4-6, 2001, pp. 532-535.

[2] Biszick, K.R., Gilbert, J.A., “Designing thin-walled, reinforced concrete panels for reverse bending," Proc. of the 1999 SEM Spring Conference on Theoretical, Experimental and Computational Mechanics, Cincinnati, Ohio, June 7-9, 1999, pp. 431-434.